Final Report of Wageningen University Contribution to FLOODsite Task 1

A. Berne, R. Uijlenhoet and P.A. Troch,
Hydrology and Quantitative Water Management Group,
Wageningen University, The Netherlands.

April 23, 2006

Contents

1 Introduction **4**

2 Travel time distributions of subsurface flow along complex hillslopes with exponential width functions **5**

2.1 Introduction 5
2.2 The hillslope-storage Boussinesq equation 6
2.2.1 Derivation of the equation 6
2.2.2 Linearization 7
2.3 Derivation of an analytical solution 8
2.3.1 Laplace transform solution 9
2.3.2 Inversion of the Laplace transform 10
2.3.3 Characterisitic dimensionless numbers 12
2.4 Travel time distribution 13
2.4.1 Derivation from the Laplace transform 13
2.4.2 Influence of the hillslope geometry 14
2.5 Conclusions 15

3 Similarity analysis of subsurface flow response of hillslopes with complex geometry **18**

3.1 Introduction 18
3.2 Dimensional analysis 20
3.2.1 General formulation 20
3.2.2 Similarity parameter: the hillslope Péclet number 22
3.3 Analytical expressions for the dimensionless CRF moments 23
3.3.1 Boundary conditions 23
3.3.2 Initial condition 1 24
3.3.3 Initial condition 2 25
3.4 Discussion 26
3.4.1 General behaviour of CRF moments as functions of Pe 26
3.4.2 Comparison with experimental data 29
3.5 Conclusions 31

4 Application to real catchments **33**

5 Conclusions **34**

6 Appendices **38**
6.1 Derivation of the dimensionless equation 38
6.2 Derivation of an analytical solution in the Laplace domain 39
6.2.1 Initial condition 1 40
6.2.2 Initial condition 2 41
6.3 Derivation of the initial steady state solution 41

Chapter 1

Introduction

The hydrological response of catchments is influenced by the lanscape characteristics. Both channel networks and hillslopes play a major role in the propagation of water within catchments, and therefore influence the generation of floods. In mountainous regions, the importance of subsurface flows has been recognized for a long time (e.g. *Dunne and Black* 1970, *Freeze* 1972a, *Beven and Kirkby* 1979). Moreover, the issue of hydrological modeling or forecasting in a context of poorly or ungauged basins adds a level of complexity by removing the possibility to calibrate hydrological models. In this report, we focus on the subsurface component of discharge at the hillslope scale (up to one km^2), and in particular on the development of a new approach providing the ability to capture the essential behaviour of the natural system using a parsimonious and computational efficient modeling. The report first presents a theoretical analysis of subsurface flow for complex hillslopes (Chapter 2 and Chapter 3), and then the first results of its application to real catchments (Chapter 4).

Chapter 2

Travel time distributions of subsurface flow along complex hillslopes with exponential width functions[1]

2.1 Introduction

Recently, the hillslope-storage Boussinesq (hsB) equation was introduced to describe subsurface flow and saturation along complex hillslopes in a simple and elegant way *Troch et al.* (2003). In its general form, the hsB equation is non-linear and the solutions presented are derived using numerical methods *Troch et al.* (2003), *Paniconi et al.* (2003). However, the equation can be linearized and then provides an interesting framework to investigate the unit flow response. Similar work has been presented concerning uniform hillslopes *Brutsaert* (1994). This chapter constitutes an attempt to generalize this approach to complex hillslopes.

First the derivation of the hsB equation is presented. Then it is linearized and the derivation of an analytical solution, by means of Laplace transforms, is described. Finally, the low order statistical moments are determined and the influence of the geometric and hydraulic characteristics of the hillslope on its hydrological unit response is investigated.

[1]Adapted version of A. Berne, R. Uijlenhoet, P. Troch and C. Paniconi, 2004: Travel time distributions of subsurface flow along complex hillslopes with exponential width functions. *XV^{th} International Conference on Computational Methods in Water Resources*, Chapel Hill, USA, pp. 1465-1477.

2.2 The hillslope-storage Boussinesq equation

2.2.1 Derivation of the equation

The main steps of the derivation of the hillslope-storage Boussinesq (hsB) equation are described in the following. The reader can refer to *Troch et al.* (2003) for more detailed explanations.

Subsurface flow along a unit-width hillslope with sloping bedrock can be described by the Boussinesq equation:

$$\frac{\partial h}{\partial t} = \frac{k}{f}\left[\cos i \,\frac{\partial}{\partial x}\left(h\frac{\partial h}{\partial x}\right) + \sin i \,\frac{\partial h}{\partial x}\right] + \frac{N}{f} \tag{2.1}$$

where $h(x,t)$ is the height of the groundwater table measured perpendicular to the underlying bedrock with a slope angle i, k is the hydraulic conductivity, f the drainable porosity, t the time and x the distance from the outlet. N is a source/sink term and corresponds to the recharge (perpendicular to the bedrock) to the groundwater table for $N > 0$. Equation (2.1) does not take into account the three-dimensional aspect of the soil mantle of the hillslope. Hence, it is not valid for hillslopes presenting a complex geometry. On the other hand, the resolution of the three-dimensional Richards' equation requires a large computational time, even for small-scale applications *Paniconi and Wood* (1993). The hsB equation has been developed to cope with the complex geometry of natural hillslopes while keeping the mathematics simple enough to limit the computational time. The derivation of the hsB equation is described below.

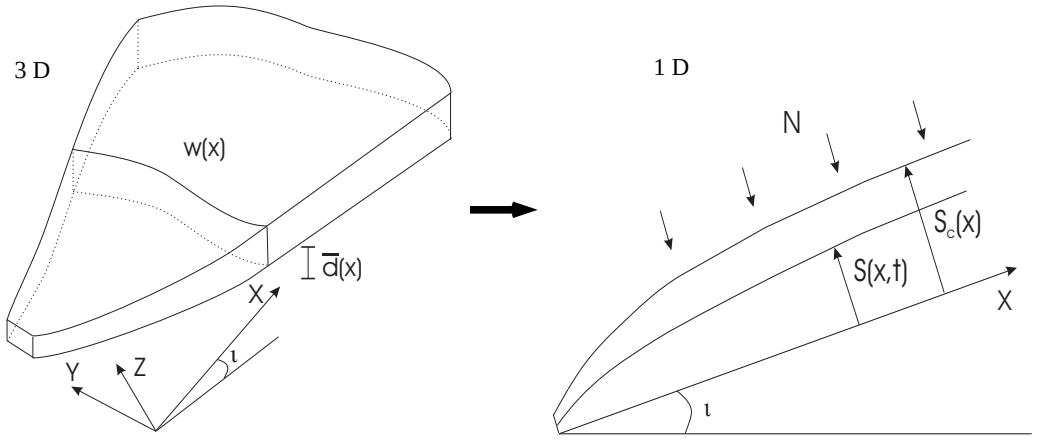

Figure 2.1: Sketch of the hsB approach.

The soil moisture storage capacity S_c has been defined in *Fan and Bras* (1998) as

$$S_c(x) = w(x)\,\bar{d}(x)\,f \tag{2.2}$$

where $w(x)$ is the width of the hillslope at a distance x and $\bar{d}(x)$ is the average soil depth at x (see Figure 2.1). S_c defines the pore space along the hillslope and accounts for both plan

shape, through the width function, and the profile curvature, through the soil depth funtion. Similarly, the soil moisture storage $S(x,t)$ has been defined in *Troch et al.* (2002) as

$$S(x,t) = w(x)\,\bar{h}(x,t)\,f \tag{2.3}$$

where $\bar{h}(x,t)$ is the average height over the width of the groundwater table at x and t. Introducing the integrated discharge over the width of the hillslope $Q(x,t)$, the continuity equation becomes

$$\frac{\partial S}{\partial t} + \frac{\partial Q}{\partial x} - Nw = 0 \tag{2.4}$$

The Darcy law can be written as

$$Q = -\frac{kS}{f}\left[\cos i\,\frac{\partial}{\partial x}\left(\frac{S}{fw}\right) + \sin i\right] \tag{2.5}$$

Combining Eqs.(2.4) and (2.5) yields the hillslope-storage Boussinesq equation:

$$f\frac{\partial S}{\partial t} = \frac{k\cos i}{f}\frac{\partial}{\partial x}\left[\frac{S}{w}\left(\frac{\partial S}{\partial x} - \frac{S}{w}\frac{\partial w}{\partial x}\right)\right] + k\sin i\frac{\partial S}{\partial x} + fNw \tag{2.6}$$

2.2.2 Linearization

Linearization is one possible approach to derive an analytical solution for Eq.(2.6) which is a non-linear partial differential equation (PDE hereafter). The non-linearity comes from the term $\frac{S}{w}$ in Eq.(2.6). Assuming the water table varies little along the hillslope, we can write:

$$\frac{S}{w} \sim p\frac{\bar{S}_c}{\bar{w}} = fp\gamma D \tag{2.7}$$

where $0 \leq p \leq 1$ is a constant introduced to compensate for the approximation coming from the linearization, $\bar{S}_c$ and $\bar{w}$ are the average storage capacity and width of the hillslope, D represents the average soil depth along the hillslope and γ expresses the initial water table height as a fraction of D. Hence $fp\gamma D$ represents the average storage per unit width along the hillslope during drainage. Substituting Eq.(2.7) in the first $\frac{S}{w}$ term of Eq.(2.6) yields:

$$f\frac{\partial S}{\partial t} = kp\gamma D\cos i\left[\frac{\partial^2 S}{\partial x^2} - \left(\frac{\partial}{\partial x}\left[\ln(w)\right]\right)\frac{\partial S}{\partial x} - \left(\frac{\partial^2}{\partial x^2}\left[\ln(w)\right]\right)S\right] + k\sin i\,\frac{\partial S}{\partial x} + fNw \tag{2.8}$$

Equation (2.8) is a linear PDE with variable coefficients.

2.3 Derivation of an analytical solution

Some coefficients of Eq.(2.8) are derivatives of $\ln(w)$. Consequently, the PDE can be further simplified by assuming an exponential form for the width function:

$$w(x) = c\, e^{ax} \tag{2.9}$$

where c corresponds to the width at the outlet ($w(0)$) and a is a shape parameter quantifying the degree of convergence ($a > 0$) or divergence ($a < 0$) of the hillslope. Therefore Eq.(2.8) can be written as

$$\frac{\partial S}{\partial t} = K \frac{\partial^2 S}{\partial x^2} + U \frac{\partial S}{\partial x} + Nw \tag{2.10}$$

where

$$K = \frac{kp\gamma D \cos i}{f}$$

and

$$U = \frac{k \sin i - akp\gamma D \cos i}{f}$$

Equation (2.10) is the classical non-stationary advection-diffusion equation. Due to the orientation of the x-axis, U must be positive for the flow direction to be towards the outlet ($x = 0$). This yields the following geometric constraint:

$$\tan i \geq ap\gamma D \tag{2.11}$$

For divergent hillslopes ($a < 0$) this inequality is always true, so there is no constraint on a, i or γD for Eq.(2.10) to be correct. On the contrary, for convergent hillslopes ($a > 0$) the slope $\tan i$ must be greater than $ap\gamma D$, or the initial water table γD must be smaller than $\frac{\tan i}{ap}$ or the width shape parameter a must be smaller than $\frac{\tan i}{p\gamma D}$.

Equation (2.10) is a linear PDE with constant coefficients and non-homogeneous forcing term. The following initial and boundary conditions are chosen:

(i)	$S(x,t) = \gamma D f\, ce^{ax}$	$x \in [0, L]$	$t = 0$
(ii)	$S(x,t) = 0$	$x = 0$	$\forall\, t > 0$
(iii)	$K\, \partial S/\partial x + US = 0$	$x = L$	$\forall\, t > 0$

Following *Brutsaert* (1994), a uniform groundwater table of $h = \gamma D$ along the hillslope is assumed as initial condition (i). The boundary condition (ii) corresponds to $h = 0$ at the outlet and the boundary condition (iii) imposes no flow at the divide of the hillslope. It is then possible to derive an analytical solution of Eq.(2.10) with the given initial and boundary conditions, using the Laplace transform.

2.3.1 Laplace transform solution

Let s denote the Laplace variable and $\widetilde{S}$ denote the Laplace transform of S with respect to time:

$$\widetilde{S}(s,x) = \int_0^\infty e^{-st} S(t,x)\, dt \tag{2.12}$$

Both N and D are finite parameters, so S is also finite. Hence the convergence of the integral is ensured. The boundary conditions (ii) and (iii) become

$$\widetilde{S}(0,s) = 0 \tag{2.13}$$

and

$$K\frac{\partial \widetilde{S}}{\partial x}(L,s) + U\widetilde{S}(L,s) = 0 \tag{2.14}$$

Equation (2.10) becomes in the Laplace domain:

$$\frac{\partial^2 \widetilde{S}}{\partial x^2} + \frac{U}{K}\frac{\partial \widetilde{S}}{\partial x} - \frac{s}{K}\widetilde{S} = -\frac{c}{K}\left(\frac{N}{s} + \gamma D f\right) e^{ax} \tag{2.15}$$

For a given s, Eq.(2.15) is a linear ordinary differential equation (ODE) with constant coefficients and non-homogeneous forcing term. The solution of such an ODE is given as the sum of the solution of the corresponding homogeneous ODE ($\widetilde{S}_h$) and a particular solution ($\widetilde{S}_p$). The homogeneous solution is given by

$$\widetilde{S}_h(x,s) = C_1\, e^{(d+b)x} + C_2\, e^{(d-b)x} \tag{2.16}$$

where

$$d = -\frac{U}{2K}$$

and

$$b = \sqrt{d^2 + \frac{s}{K}}$$

C_1 and C_2 are integration constants, fixed by the boundary conditions. The particular solution can be derived using the method of variation of parameters *Boyce and DiPrima* (1977):

$$\widetilde{S}_p(x,s) = -\frac{c\,(N + s\gamma D f)}{s\,(Ka^2 + Ua - s)}\, e^{ax} \tag{2.17}$$

Finally, the general solution of Eq.(2.10) is:

$$\widetilde{S}(x,s) = C_1 e^{(d+b)x} + C_2 e^{(d-b)x} - \frac{c\,(N + s\gamma D f)}{s\,(Ka^2 + Ua - s)}\, e^{ax} \tag{2.18}$$

where C_1 and C_2 are determined in order to fulfill the boundary conditions (2.13) and (2.14):

$$C_1 = \frac{c\,(N + s\gamma Df)}{s\,(Ka^2 + Ua - s)} \frac{e^{aL}\,(a - 2d) + e^{(d-b)L}\,(d + b)}{2e^{dL}\,[b\,\cosh(bL) - d\,\sinh(bL)]}$$

$$C_2 = \frac{c\,(N + s\gamma Df)}{s\,(Ka^2 + Ua - s)} \frac{e^{(d+b)L}\,(b - d) - e^{aL}\,(a - 2d)}{2e^{dL}\,[b\,\cosh(bL) - d\,\sinh(bL)]}$$

We now have the analytical expression of the storage in the Laplace domain, which must be inverted to obtain the function describing the storage in the time domain, along the hillslope.

2.3.2 Inversion of the Laplace transform

The inverse Laplace transform of $\widetilde{S}$ is defined by

$$L^{-1}\{\widetilde{S}(s,x)\} = \lim_{v \to +\infty} \frac{1}{2i\pi} \int_{u-iv}^{u+iv} \widetilde{S}(s,x) e^{st}\, ds \tag{2.19}$$

The convergence of the integral has been verified. According to the residues theorem, this integral can be evaluated as the sum of the residues at the poles of $\widetilde{S}(s,x)e^{st}$. For the clarity and the shortness of this chapter, the detailed calculations are not described (see *Troch et al.* (2004)). The final analytical expression for S is:

$$S(x,t) = \sum_{n=0}^{+\infty} \left\{ \frac{2dL^2 c z_n \left[e^{dL} \left(\frac{z_n}{L} \sin(z_n) + d\cos(z_n) \right) + (a - 2d) e^{aL} \right]}{\cos(z_n)\,(-dL + z_n^2 + d^2L^2)\,(a^2L^2 - 2daL^2 + z_n^2 + d^2L^2)} \sin\left(\frac{z_n x}{L}\right) \right.$$
$$\left. \times \left[\gamma D f e^{s_n t - d(L-x)} + \frac{N}{s_n} e^{-d(L-x)} \left(e^{s_n t} - 1 \right) \right] \right\} \tag{2.20}$$

where

$$\frac{z_n}{dL} = \tan(z_n)$$

and

$$s_n = -K \left(\frac{z_n^2}{L^2} + d^2 \right)$$

Applying the continuity equation for $x = 0$ enables to derive the drainage flux:

$$Q(0,t) = -K \left[\frac{\partial S}{\partial x} \right]_{x=0} \quad \Leftrightarrow$$

$$Q(0,t) = \sum_{n=0}^{+\infty} \left\{ (\gamma D f s_n + N) \frac{2dL^2 c z_n \left[e^{dL} \left(\frac{z_n}{L} \sin(z_n) + d\cos(z_n) \right) + (a - 2d) e^{aL} \right] e^{s_n t - dL}}{\cos(z_n)\,(-dL + z_n^2 + d^2L^2)\,(a^2L^2 - 2daL^2 + z_n^2 + d^2L^2)} \right.$$
$$\left. \times \frac{L z_n}{z_n^2 + d^2 L^2} \right\} - \frac{Nc}{a} \left(e^{aL} - 1 \right) \tag{2.21}$$

Figure 2.2 displays the total storage over the hillslope and the subsurface flow at the outlet for zero recharge ($N = 0$), for a convergent, a uniform and a divergent hillslope and for the hillslope parameters given in Table 2.1. The corresponding total volumes, mean travel times and standard deviations are given in Table 2.2. The discharge peak at $t = 0$ is due to the initial condition assumed for S ($S(x, 0) = \gamma D f c e^{ax}$). It has been verified that its influence on the moments of the distribution is negligible.

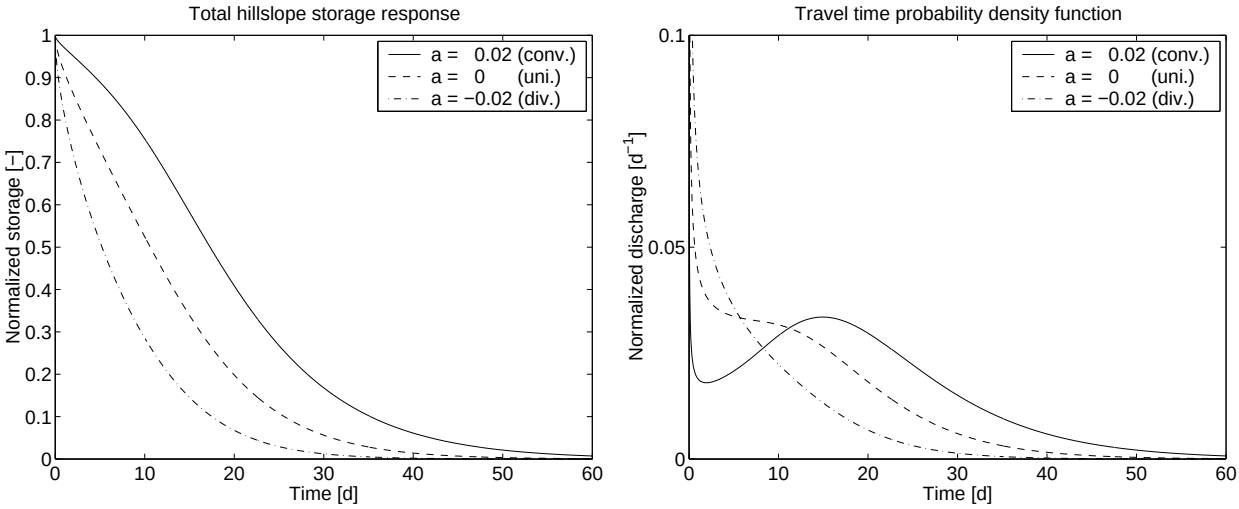

Figure 2.2: Left: total storage over the hillslope, normalized by the total volume. Right: discharge at the outlet, normalized by the total volume. The solid line corresponds to a convergent hillslope ($a > 0$), the dashed to a uniform hillslope ($a = 0$) and the dashed-dotted to a divergent hillslope ($a < 0$).

Table 2.1: Hillslope characteristics.

Drainable porosity	f	0.3	-
Hydraulic conductivity	k	24	m·day^{-1}
Length	L	100	m
Soil depth	D	2	m
Initial height ratio	γ	0.2	-
Linearization parameter	p	1	-
Slope angle	i	0.05	rad
Width at the outlet	c	10	m

Table 2.2: Travel time distribution statistics.

Moment	Conv.	Unif.	Div.
Volume (m^3)	383	120	52
Mean (day)	19.0	12.4	7.4
σ (day)	12.4	9.8	7.3

2.3.3 Characterisitic dimensionless numbers

Dimensionless numbers taking into account the geometric and hydraulic aspects of the hillslope characterize the PDE (2.10) and the analytical solution (2.20). For uniform hillslopes, $\frac{LU}{2K} = \frac{L}{2p\gamma D} \times \tan i$ appears as a dimensionless characteristic number *Brutsaert* (1994). It can be interpreted as the relative magnitude of gravity drainage versus diffusion drainage. For complex hillslopes, this number becomes:

$$\frac{LU}{2K} = \frac{L}{2p\gamma D} \tan i - \frac{aL}{2} \tag{2.22}$$

The top view plan shape of the hillslope $\frac{aL}{2}$ appears as a second dimensionless number. For uniform hillslopes ($a = 0$), Eq.(2.22) reduces to the definition proposed in *Brutsaert* (1994). For convergent hillslopes ($a > 0$), the value of the dimensionless number decreases compared to a uniform hillslope of similar geometry (i, D and L) by the term $\frac{aL}{2}$ which depends on the degree of convergence. It shows the necessity to take into account the diffusion effects in the hydrological modelling of a hillslope response. In a similar way, the dimensionless parameter increases for a divergent hillslope ($a < 0$), showing that the advection effects become more and more important and eventually the kinematic wave approximation becomes valid. Finally, it must be underlined that these two dimensionless numbers are independent of both the porosity and the hydraulic conductivity of the hillslope.

In groundwater transport studies the dimensionless number previously defined is also referred to as the Péclet number (Pe). Pe represents the ratio of the time scales of dispersive and advective transport from the middle of the hillslope:

$$\mathrm{Pe} = \frac{LU}{2K} = \frac{\frac{(L/2)^2}{K}}{\frac{(L/2)}{U}} = \frac{\tau_K}{\tau_U}$$

The characteristic dispersive time is

$$\tau_K = \frac{L^2}{4K} = \frac{L^2 f}{4kp\gamma D \sin i} \tag{2.23}$$

and the characteristic advective time is

$$\tau_U = \frac{L}{2U} = \frac{Lf}{2\left(k \sin i - akp\gamma D \cos i\right)} \tag{2.24}$$

Only the latter depends on the plan shape of the hillslope viz the coefficient a. The constraint (2.11) implies $\tau_U > 0$. The characteristic advective time is larger for a convergent hillslope ($a > 0$) than for a divergent one ($a < 0$). It means that the advection is more important for a divergent hillslope (all other parameters being fixed).

2.4 Travel time distribution

2.4.1 Derivation from the Laplace transform

The hydrograph corresponding to the pure drainage of a hillslope can be seen as the groundwater unit response. Moreover, the hydrograph (normalised by the total volume) represents the probability density function (pdf) of the travel times along the hillslope. The low order moments provide relevant information to characterize a distribution. An analytical expression of these moments enables to directly analyse the influence of the hillslope parameters (geometric and hydraulic) on the distribution.A study of the three first moments of the travel time distribution along a uniform hillslope has been presented in *Brutsaert* (1994). In this section this approach is generalized to more complex hillslopes with exponential width functions, still based on the properties of the Laplace transform.

Indeed, the Laplace transform has an interesting property concerning the moments:

$$\frac{d^n L\{f\}}{ds^n}(0) = (-1)^n \int_0^\infty t^n f(t)\, dt = (-1)^n\, m_n(f) \tag{2.25}$$

where f represents a pdf and $L\{f\}$ is its Laplace transform. $m_n(f)$ corresponds to the n$^{\text{th}}$ order moment of the pdf. In the statistical literature, the Laplace transform of a pdf is known as its moment generating function *Mood et al.* (1974).

The analytical expression of the Laplace transform of the discharge is convenient to study the moments of the travel time distribution. Combining the Laplace transform of the continuity equation (2.4) with $N = 0$ (pure drainage), the analytical expression of $\widetilde{S}$ given in Eq.(2.18) and the boundary condition (2.14), the Laplace transform of the discharge $\widetilde{Q}$ reads:

$$\begin{aligned}
\widetilde{Q}(x,s) &= -K\frac{\partial \widetilde{S}(x,s)}{\partial x} - U\widetilde{S}(x,s) \quad \Leftrightarrow \\
\widetilde{Q}(x,s) &= \frac{c\gamma D f}{(Ka^2 + Ua - s)} e^{ax}\left(Ka + U\right) - C_1 e^{(d+b)x}\left[K\left(d+b\right) + U\right] \\
&\quad - C_2 e^{(d-b)x}\left[K\left(d-b\right) + U\right]
\end{aligned} \tag{2.26}$$

C_1 and C_2 are the same constants as in Eq.(2.18). To represent a pdf, Q must be normalized by the total volume of flow m_0 which has passed through the hillslope at x when $t \to \infty$:

$$m_0(x) = |\widetilde{Q}(x,0)| = \frac{c\gamma D f}{a}\left(e^{aL} - e^{ax}\right) \tag{2.27}$$

It must be noted that $Q(x,t)$ is negative because of the orientation of the x-axis (increasing up the slope). Consequently $m_0(x)$ is taken as $|\widetilde{Q}(x,0)|$ to represent the total volume of the flow.

On the other hand, the total volume can be seen as the integral of the initial water table along the considered part of the hillslope:

$$\int_x^L \gamma D f w(u)\, du = \frac{c\gamma D f}{a}\left(e^{aL} - e^{ax}\right) \tag{2.28}$$

This shows the consistency of the expression derived for $\widetilde{S}$ and $\widetilde{Q}$. Taking $a = 0$ (uniform hillslope), we find $m_0(x) = c\gamma D f\,(L - x)$, which is consistent with Eq.(23) in *Brutsaert* (1994) choosing $\gamma = 1$ and $c = 1$.

Due to the complexity of the derivations, we shall analyze only the moments at the outlet of the hillslope ($x = 0$). The first order moment m_1 corresponds to the mean travel time:

$$m_1 = \frac{L^2}{K}\frac{1}{aL\,(aL + 2\mathrm{Pe})\,(e^{aL} - 1)} \times \left\{1 + \frac{aL}{2\mathrm{Pe}}\left(1 - e^{-2\mathrm{Pe}}\right) + e^{aL}\left[aL - 1 + \frac{aL}{2\mathrm{Pe}}\left(aL - 1 - \frac{aL}{2\mathrm{Pe}}\right)\right] + aL\left(1 + \frac{aL}{2\mathrm{Pe}}\frac{e^{aL-2\mathrm{Pe}}}{2\mathrm{Pe}}\right)\right\} \tag{2.29}$$

and

$$\lim_{a\to 0} m_1 = \frac{L^2}{8K}\frac{1}{\mathrm{Pe}^2}\left[2\mathrm{Pe}^2 - 1 + (2\mathrm{Pe} + 1)\, e^{-2\mathrm{Pe}}\right]$$

which is consistent with Eq.(24) in *Brutsaert* (1994). The first moment represents a time and can not be expressed as a function of dimensionless numbers. It can be normalized by the dispersive characteristic time τ_K when $\mathrm{Pe} \to 0$ and by the advective characteristic time τ_U when $\mathrm{Pe} \to \infty$.

The analytical expressions of the higher order moments are too long to be presented in this chapter. It must be noted that it is possible to define dimensionless numbers related to the higher order moments (for example the coefficent of variation, the skewness and the kurtosis excess), depending only on the dimensionless numbers $\mathrm{Pe} = \frac{LU}{2K}$ and $\frac{aL}{2}$.

It is interesting to note that the drainable porosity f and the hydraulic conductivity k only influence the total volume and the mean travel time. The higher order normalized moments depend only on the geometry of the hillslope. These conclusions are restricted to the domain of validity of the linearized equation.

2.4.2 Influence of the hillslope geometry

The analytical expressions of the moments enable to study the influence of the geometric and hydraulic characteristics of the hillslope on the travel time distribution.

According to Eq.(2.29), m_1 is independent of the width c and is proportional to $\frac{L^2}{K}$. For all other variables fixed, m_1 is then proportional to f and to k^{-1}. Concerning the influence of the geometric characteristics of the hillslope, we limit our analysis to the slope angle i and the width shape parameter a, while all other variables are fixed (see Table 2.1). Figure 2.3 displays m_1 as a function of i and a respectively. The mean travel time decreases when the slope angle increases for both convergent and divergent hillslopes. So when Pe increases and K decreases, the mean travel time m_1 decreases. As Pe increases and K decreases when γD decreases, it shows that the mean travel time decreases when the initial water height γD decreases. Similarly, the mean travel time decreases when the width shape parameter decreases for any slope angle. It shows that convergent hillslopes ($a > 0$) have a significantly larger mean travel time than the divergent hillslopes.

The coefficient of variation (CV hereafter) is a dimensionless second order moment, function of Pe and $\frac{aL}{2}$. Pe is the difference between $(\frac{L}{2p\gamma D} \times \tan i)$ and $\frac{aL}{2}$, which are independent dimensionless numbers. $(\frac{L}{2p\gamma D} \times \tan i)$ characterizes the side view plan shape of the hillslope: $\frac{L}{2p\gamma D}$ is the ratio of the half length and the depth of the soil mantle; $\tan i$ is the slope. $\frac{aL}{2}$ characterizes the top view plan shape of the hillslope. Figure 2.4 displays the CV of the travel time distribution as a function of $(\frac{L}{2p\gamma D} \times \tan i)$ and $\frac{aL}{2}$ respectively. As pointed out before, U (and so Pe) must be positive and so $(\frac{L}{2p\gamma D} \times \tan i)$ must be greater than $\frac{aL}{2}$. CV decreases when $(\frac{L}{2p\gamma D} \times \tan i)$ increases, which corresponds either to a more shallow soil mantle or to a steeper hillslope. CV decreases when $\frac{aL}{2}$ increases, which corresponds to a wider convergent hillslope if $a > 0$ or to a more narrow divergent one if $a < 0$. However, the standard deviation σ (for the given values of the hillslope variables) decreases also with $\frac{aL}{2}$, but more slowly than the mean (see Table 2.2). It explains the increase of CV when $\frac{aL}{2}$ decreases.

These results show that the mean travel time and the variability decrease when the flow is confined to more shallow or steeper hillslopes (decrease of the mean and CV when the slope angle and $\frac{L}{2p\gamma D}$ increase) and when the hillslope boundaries have less effects (decrease of the mean and σ when the width shape parameter and $\frac{aL}{2}$ decrease). According to these results, the diffusion effects increase the mean and the variability of the travel time distribution of the subsurface flow in a hillslope.

2.5 Conclusions

Introducing the width function and the groundwater storage of the hillslope in the Boussinesq equation leads to the hillslope-storage Boussinesq equation (hsB). This equation describes the diffusion and advection components of the subsurface flow and takes the three-dimensional aspect of the hillslope explicitly into account.

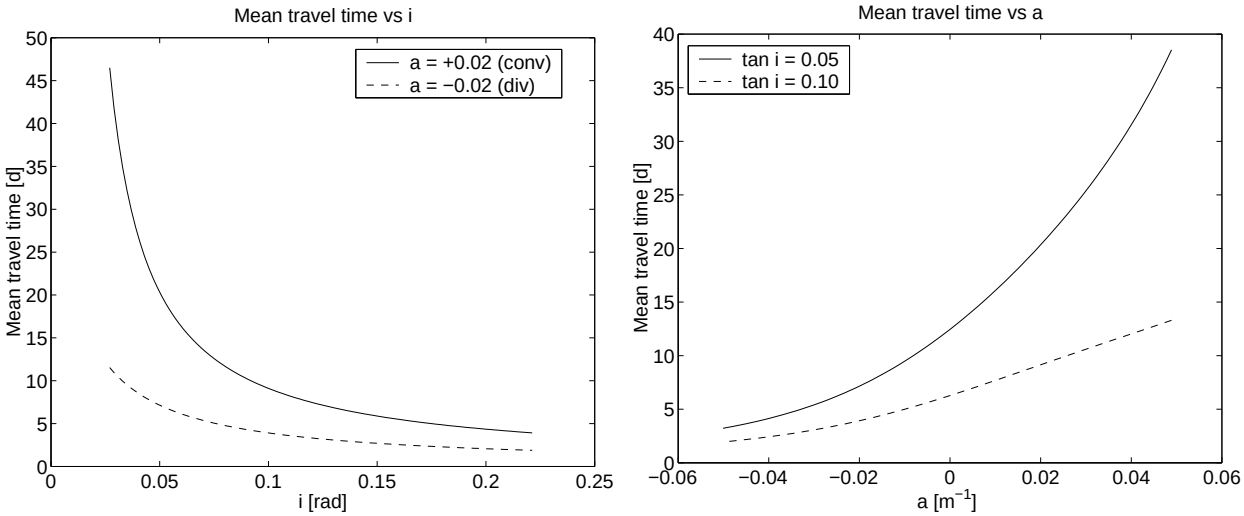

Figure 2.3: Left: influence of the slope angle i on the mean travel time, for a convergent ($a = 0.02\,\mathrm{m}^{-1}$) and a divergent hillslope ($a = -0.02\,\mathrm{m}^{-1}$). Right: influence of the width shape parameter a on the mean travel time, for two slopes (5 and 10%).

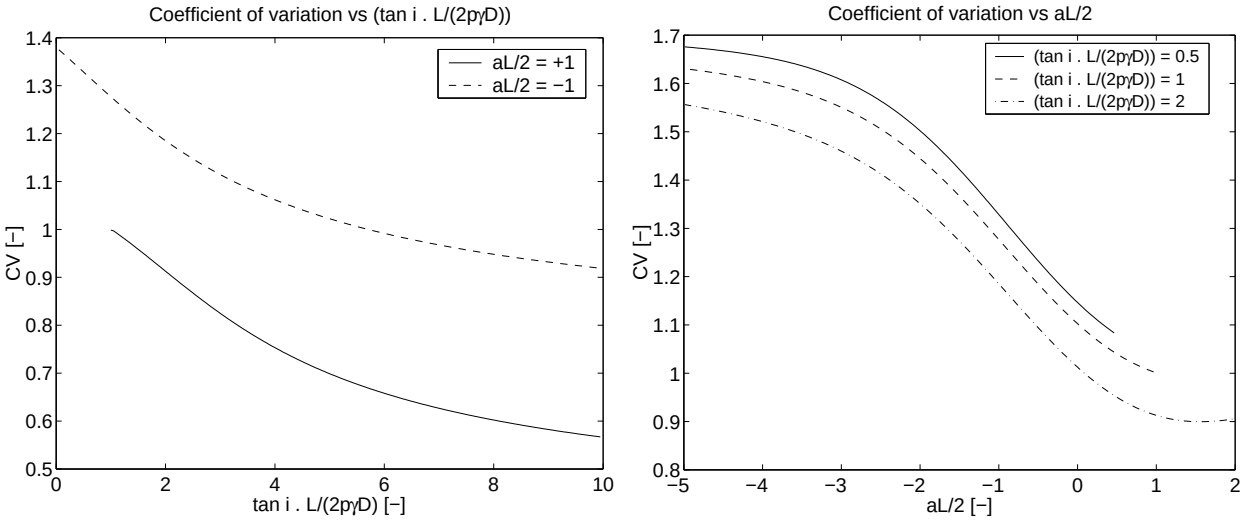

Figure 2.4: Left: influence of $(\frac{L}{2p\gamma D} \times \tan i)$ on the coefficient of variation of the travel time distribution, for a convergent ($\frac{aL}{2} = 1$) and a divergent hillslope ($\frac{aL}{2} = -1$). Right: influence of $\frac{aL}{2}$ on the coefficient of variation of the travel time distribution, for $(\frac{L}{2p\gamma D} \times \tan i) = 0.5$, 1 and 2.

The hsB equation has been linearized and an analytical solution has been derived using Laplace transforms, following the approach proposed in *Brutsaert* (1994). Two independent dimensionless geometric numbers characterize the solution: (i) $(\frac{L}{2p\gamma D} \times \tan i)$ representing the side view shape and (ii) $(\frac{aL}{2})$ representing the top view shape of the hillslope.

The Laplace transform of a probability density function is its statistical moment generating function. The low order moments of the travel time distribution have been analysed with respect to the hillslope geometric and hydraulic characteristics. The diffusion effects are significant for low sloping and converging hillslopes. They increase the mean travel time and the variability of the hillslope unit response.

Further investigations are required to study the influence of the initial conditions assumed and to take into time-dependent account recharge.

Chapter 3

Similarity analysis of subsurface flow response of hillslopes with complex geometry[1]

3.1 Introduction

Landscape geomorphology (hillslope geometry) and pedology (soil properties) influence the hydrological response of catchments. Thus, clear insight into the effect of the shape and hydraulic characteristics of landscape elements is required to further our understanding of and our ability to model catchment hydrological processes. For some time, research has focused on identifying and quantifying hillslope processes as a first step towards assessment of (sub)catchment response. In hilly catchments the importance of subsurface flow processes in generating variable source areas was first addressed by *Dunne and Black* (1970) and *Freeze* (1972a;b). The idea that landscape structure is a dominant control of the hydrological behaviour, and that hydrological models therefore should take this structure explicitly into account has already a long tradition in hydrology. For example, *Beven and Kirkby* (1979) showed how geomorphometric parameters can be used to describe the hydrological behaviour at a given position within the landscape, while *Rodríguez-Iturbe and Valdés* (1979) showed how the shape of a catchment unit hydrograph can be explained from the structure of the channel network. However, the role of geomorphological characteristics of individual hillslopes and their effect on runoff generation has received less attention.

There is hence a need for quantifying the hillslope hydrological processes and for the development of appropriate models to describe these processes. Several models have been developed

[1]Adapted version of A. Berne, R. Uijlenhoet and P. Troch, 2005: Similarity analysis of the subsurface flow response of hillslopes with complex geometry. *Water Resources Research*, 41, W09410, doi:10.1029/2004/WR003629.

over the past 30 years. The most complete models involve numerically solving the three-dimensional Richard's equation for complex hillslope geometries (*Paniconi and Wood* 1993, *Bronstert* 1994). To overcome difficulties associated with 3D models (parameterization, computational demands), a series of low-dimensional hillslope models has recently been developed (*Fan and Bras* 1998, *Troch et al.* 2003). These models are called hillslope-storage dynamics models and are able to treat the three-dimensional structure of hillslopes in a simple way, resulting in a significant reduction of model complexity. *Troch et al.* (2003) and *Hilberts et al.* (2004) demonstrated that (numerical) solutions of the 1D hillslope-storage Boussinesq (hsB) equation account explicitly for plan shape (by means of the hillslope width function) and profile curvature (local bedrock slope angle and hillslope soil depth function) of the hillslope. Recently, *Troch et al.* (2004) presented an analytical solution of the linearized hsB equation for exponential hillslope width functions. Analytical solutions like these provide essential insights in the functioning of hillslopes and may form the basis of hillslope similarity analysis (*Brutsaert* 1994).

The search for hydrological similarity indices to classify catchments based on soil, topography, vegetation and climate characteristics has been a very active research topic over the past decades (e.g. *Hebson and Wood* 1986, *Sivapalan et al.* 1987; 1990, *Saleem and Salvucci* 2004), but definitive conclusions on similarity behaviour of landscapes, based on similarity of dominant hillslope processes, have not yet been achieved. This is mainly explained by the lack of analytical relations between the flow processes and the landscape characteristics (*Aryal et al.* 2002). Analytical solutions for subsurface flow in (complex) hillslopes provide a link between the physics of the subsurface flow processes and the hillslope geometric and hydraulic properties, and therefore are useful tools to understand landscape hydrological similarity. In this chapter, we focus on groundwater flow and other hydrological processes (e.g. macropore or overland flow) are not considered.

Brutsaert (1994) derived an analytical solution to a linearized Boussinesq equation to study the hillslope subsurface flow unit response, corresponding to the free drainage of an unconfined aquifer. The motivation for his work was to provide a direct link between the underlying physical mechanisms of hillslope subsurface flow and the general linear theory of catchment hydrology (*Dooge* 1973). The analytical approach provides a powerful framework to analyze the influence of the different characteristics (hydraulic and geometric) of the hillslope on the shape of its hydrological response. In linear systems theory, the unit response function of a spatially lumped system (e.g. a linear reservoir) completely describes its dynamics. For a spatially distributed linear system with specified boundary conditions, the characteristic response is also influenced by the initial conditions (e.g. *Chapman* 1995): the way a given volume of water is initially distributed within an aquifer of finite length will influence its drainage. To describe the subsurface flow response of a hillslope, we define the characteristic response function (CRF hereafter) as the free drainage discharge normalized by the total outflow volume (for given initial and boundary conditions). The normalization allows to compare different hillslopes.

The main objective of our approach is to link subsurface flow dynamics to the geometric and hydraulic characteristics of the hillslope, by means of a similarity analysis. The hillslope hydrological response will be studied through the moments of the CRF. Since we are interested in deriving explicit relations between hillslope aquifer properties and the characteristic response, we seek to separate the effects of the boundary and initial conditions and the effects of the hillslope geometric and hydraulic properties on the moments of the CRF. A dimensional analysis of a linearized hsB equation and the obtained hydrological similarity parameter are presented in section 3.2. The derivation of the analytical expressions of the CRF moments for two different types of initial conditions is given in section 3.3. In section 3.4, the dimensionless moments of the CRF are analyzed and compared with empirical moments estimated from laboratory hillslope outflow measurements. Finally our conclusions are presented in section 3.5.

3.2 Dimensional analysis

3.2.1 General formulation

Our starting point is equation (16) in *Troch et al.* (2003), which describes the evolution of the saturated soil water storage $S = fw\bar{h}$ (where f is the drainable porosity, w is the hillslope width function and $\bar{h}$ is the average groundwater table height, perpendicularly to the bedrock, over the width) along a hillslope with an exponential width function $w(x) = ce^{ax}$ (see Figure 3.1):

$$\frac{\partial S}{\partial t} = K \frac{\partial^2 S}{\partial x^2} + U \frac{\partial S}{\partial x} + Nw \tag{3.1}$$

with

$$\begin{aligned} K &= \frac{kpD\cos\alpha}{f} \\ U &= \frac{k\sin\alpha}{f} - aK \end{aligned}$$

where x is the distance from the outlet of the hillslope, t is time, k is the hydraulic conductivity, D is the soil depth, α is the slope of the bedrock, p is a linearization parameter and N is the recharge to the groundwater table. The main assumptions for the validity of (3.1) are a shallow soil mantle, stream lines parallel to an impervious bedrock, a negligible influence of the unsaturated zone, a constant slope angle and a uniform hydraulic conductivity. These are common assumptions in hillslope hydrology (*Brutsaert* 1994) and we are convinced that analytical solutions of (3.1) provide useful insights into the hydrological response of individual hillslopes. Equation (3.1) is the classical linear non-stationary advection-diffusion equation for which analytical solutions can be derived given suitable boundary and initial conditions as well as a suitable recharge rate. In the following, advection and diffusion refer to the transport of water due to total head gradients and should not be confused with advection and diffusion in

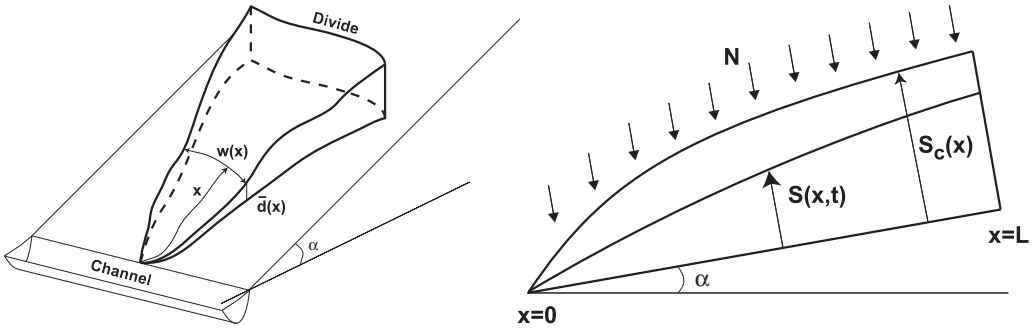

Figure 3.1: Hillslope conceptualization and definition of the storage (from *Troch et al.* 2003).

solute transport. The integrated discharge Q over the hillslope width is

$$Q = -K\frac{\partial S}{\partial x} - US \tag{3.2}$$

Hereafter, we shall consider Q to be negative and U to be positive, so that the flow is towards the outlet. The signs are defined by the x-axis orientation (see Figure 3.1). The assumption that U must be positive leads to the following geometric constraint:

$$\tan\alpha > apD \tag{3.3}$$

For divergent hillslopes ($a < 0$) this inequality is always true, so there is no constraint on a, α or pD. On the contrary, for convergent hillslopes ($a > 0$) the constraint on the degree of convergence is $a < \tan\alpha/(pD)$.

We consider the free drainage of a hillslope, i.e. $N = 0$, given specific initial conditions (see section 3.3). In the Laplace domain, the partial differential equation (3.1) becomes an ordinary differential equation (ODE):

$$K\frac{\partial^2 \widetilde{S}}{\partial x^2} + U\frac{\partial \widetilde{S}}{\partial x} - s\widetilde{S} = -S_0 \tag{3.4}$$

where $\widetilde{S}$ is the Laplace transform of S (see equation 6.2 in appendix 6.1), s is the Laplace variable and S_0 denotes the assumed initial condition. From (3.4) it is possible to derive an analytical expression for $\widetilde{S}$ and hence for $\widetilde{Q}$, the Laplace transform of Q. As $\widetilde{Q}$ (normalized by the total input volume) is the moment generating function of the CRF (e.g. *Brutsaert* 1994), we analyze the CRF through its moments to avoid the difficult transformation back to the time domain (e.g. *Troch et al.* 2004).

In order to derive similarity parameters for the CRF, a dimensional analysis is conducted. We have to define characteristic values for the dimensions involved in (3.4), *i.e.* length and

time. We use half of the hillslope length ($\frac{L}{2}$) to normalize the length dimension. From (3.1), we define the characteristic diffusive time from the middle of the hillslope as $\tau_K = L^2/(4K)$. We use τ_K to normalize the time dimension (see section 3.2.2). The dimensionless form of (3.4) reads

$$\frac{\partial^2 \widetilde{S}^*}{\partial {x^*}^2} + \frac{UL}{2K}\frac{\partial \widetilde{S}^*}{\partial x^*} - s^* \widetilde{S}^* = -S_0^* \tag{3.5}$$

where the asterisk denotes a dimensionless variable. We can derive a general formulation for the dimensionless CRF moments (see Appendix 6.1):

$$m_n^* = \phi_n \left(\frac{UL}{2K}, \pi^* \right) \tag{3.6}$$

where m_n^* denotes the dimensionless n$^{\text{th}}$ order moment of the CRF, ϕ_n is a function of dimensionless variables and π^* represents a set of dimensionless variables linked to the boundary and initial conditions. The dimensionless central moments are then given by:

$$\mu_n^* = \sum_{k=0}^{k=n} (-1)^{n-k} \binom{n}{k} m_k^* \, {m_1^*}^{n-k} \tag{3.7}$$

where $\binom{n}{k}$ represents the binomial coefficient. The dimensional moments m_n and μ_n are obtained by multiplying m_n^* and μ_n^* by τ_K^n. Equations (3.6) and (3.7) provide dimensionless expressions for the CRF moments and therefore can be used to perform a similarity analysis. A dimensional analysis can also be conducted by means of Buckingham's pi theorem (*Buckingham* 1914). However, such an analysis is independent of the form of (3.1) and will not allow to separate in an effective and objective manner the effects of the hillslope geometric and hydraulic properties from effects of the boundary and initial conditions and is therefore not conducted here.

3.2.2 Similarity parameter: the hillslope Péclet number

From (3.6) we see that the dimensionless CRF moments depend on the dimensionless number $UL/(2K)$. Together with the π^* terms, this dimensionless number defines the normalized hillslope hydrological response. We therefore propose to use $UL/(2K)$ as the subsurface flow similarity parameter for complex hillslopes. This number can be interpreted as the ratio between the characteristic diffusive time and the characteristic advective time, defined for the middle of the hillslope (e.g. *Kirchner et al.* 2001), and therefore is called hereafter the hillslope Péclet number for subsurface flow:

$$\mathrm{Pe} = \frac{\tau_K}{\tau_U} = \frac{\frac{(L/2)^2}{K}}{\frac{(L/2)}{U}} = \frac{UL}{2K} = \left(\frac{L}{2pD} \right) \tan\alpha - \left(\frac{aL}{2} \right) \tag{3.8}$$

where the characteristic advective time is

$$\tau_U = \frac{L}{2U} = \frac{Lf}{2k\left(\sin\alpha - apD\cos\alpha\right)} \tag{3.9}$$

and the characteristic diffusive time is

$$\tau_K = \frac{L^2}{4K} = \left(\frac{fL}{2k}\right)\left(\frac{L}{2pD}\right)\left(\frac{1}{\cos\alpha}\right) \tag{3.10}$$

The characteristic diffusive time τ_K is used to normalize the time dimension because it does not approach infinity when Pe approaches 0, as opposed to τ_U. Equation (3.3) guarantees that τ_U, and hence Pe, is always defined and positive. From (3.8) we can see that Pe is a function of three independent dimensionless numbers: $L/(2pD)$, $\tan\alpha$ and $aL/2$; $L/(2pD)$ represents the ratio of the half length and the average depth of the aquifer, and $\tan\alpha$ represents the slope of the bedrock. Their product characterizes the vertical geometry of the aquifer, while $aL/2$ characterizes the planar geometry of the aquifer. When $[L/(2pD) \times \tan\alpha]$ decreases or $aL/2$ increases, Pe decreases. This means that the storage gradients become stronger and therefore the contribution of the diffusion term in (3.1) increases. Note that for a uniform hillslope ($a = 0$), (3.8) reduces to the dimensionless parameter given in *Brutsaert* (1994, equation 28).

In addition to the influence of the initial and boundary conditions (see section 3.4), the dimensionless number Pe defines the hydrological similarity between hillslopes with respect to their characteristic response.

3.3 Analytical expressions for the dimensionless CRF moments

In section 3.2, a general formulation for the moments of the CRF has been derived. This section is devoted to the derivation of analytical expressions for these moments for two different types of initial conditions. In this manner, explicit relations between the hydraulic and geometric properties of the hillslope and its subsurface flow response are obtained. We have to solve (3.5) to derive an analytical expression for the dimensionless Laplace transform of the discharge $\widetilde{Q}^*$ and use it as the CRF moment generating function. The first step is to define the boundary and initial conditions that will be used to solve the differential equation.

3.3.1 Boundary conditions

Equation (3.5) will be solved with the following boundary conditions commonly used in hillslope hydrology (e.g. *Brutsaert* 1994, *Verhoest and Troch* 2000, *Troch et al.* 2004): (i) assuming the groundwater table height at the outlet to be small in comparison to the mean groundwater table height along the hillslope, we impose the storage to be zero at the outlet; (ii) the uphill boundary of the hillslope coincides with the catchment divide, and we assume the flow through the divide to be zero. In a dimensionless form and in the Laplace domain, these boundary

conditions are expressed as

$$\begin{aligned} &\widetilde{S}^* = 0 && x^* = 0 && \forall t \geq 0 \\ &\frac{\partial \widetilde{S}^*}{\partial x^*} + \mathrm{Pe}\widetilde{S}^* = 0 && x^* = 2 && \forall t \geq 0 \end{aligned} \tag{3.11}$$

It must be noted that these boundary conditions do not require other numbers than Pe to be described in a dimensionless way. Therefore π^* will only depend on the initial condition in this case.

3.3.2 Initial condition 1

The first type of initial condition corresponds to a storage profile defined as a fraction γ of the storage capacity $S_c = fwD$ (*Troch et al.* 2004):

$$S_0(x) = \gamma D f w(x) = \left(\frac{L}{2}\right)^2 \frac{4\gamma D f c}{L^2} e^{ax} \qquad \forall x \in [0, L] \tag{3.12}$$

where $\gamma \in [0, 1]$ is a factor defining the initial groundwater table height as a fraction of the soil depth D. If the soil depth is constant along the hillslope, then the initial groundwater table height (γD) is also constant along the hillslope. The dimensionless initial storage profile is given by

$$S_0^*(x^*) = \frac{4\gamma D f c}{L^2} e^{\frac{aL}{2}x^*} \tag{3.13}$$

Therefore the parameter set π_0^*, representing the initial condition, is $\{\frac{4\gamma D f c}{L^2}; \frac{aL}{2}\}$. However, $\frac{4\gamma D f c}{L^2}$ is a proportionality factor for S_0^*. Because of the linearity of (3.2) and (3.4), it will also be a proportionality factor for $\widetilde{Q}^*$. Hence, this factor will disappear in the expression for the dimensionless CRF moments and as a consequence π_0^* reduces to $\pi^* = \{\frac{aL}{2}\}$. It must be noted that this initial storage profile does not satisfy the imposed boundary condition at the outlet for $t = 0$.

The obtained expression for the dimensionless discharge in the Laplace domain is (see Appendix 6.2.1)

$$\begin{aligned} \widetilde{Q}^*(s^*, x^*) = &- \frac{8\gamma D f c}{L^2} \frac{1}{(aL(aL + 2\mathrm{Pe}) - 4s^*)} \Bigg\{ - e^{\frac{aL}{2}x^*} (aL + 2\mathrm{Pe}) \\ &+ \frac{4s^* \left[e^{(d-b)L} e^{\frac{L(d+b)}{2}x^*} - e^{(d+b)L} e^{\frac{L(d-b)}{2}x^*} \right]}{L\left[(b-d)\, e^{(d+b)L} + (b+d)\, e^{(d-b)L}\right]} \\ &+ \frac{(aL + 2\mathrm{Pe})\, L e^{aL} \left[(b-d)\, e^{\frac{L(d+b)}{2}x^*} + (b+d)\, e^{\frac{L(d-b)}{2}x^*} \right]}{L\left[(b-d)\, e^{(d+b)L} + (b+d)\, e^{(d-b)L}\right]} \Bigg\} \end{aligned} \tag{3.14}$$

where $dL = -\text{Pe}$ and $bL = \sqrt{Pe^2 + 4s^*}$. The dimensionless total initial volume uphill of the outlet ($x^* = 0$) is

$$V^* = -\widetilde{Q}^*(0,0) = \frac{8\gamma Dfc}{aL^3}\left(e^{aL} - 1\right) \tag{3.15}$$

Integrating (3.13) between $x^* = 0$ and $x^* = 2$ yields the same expression. Taking the first derivative of (3.14) with respect to s^* for $s^* = 0$ at the outlet and normalizing by (3.15) yields the first dimensionless CRF moment (i.e. the normalized mean response time):

$$m_1^* = \frac{4}{aL\left(aL + 2\text{Pe}\right)\left(e^{aL} - 1\right)} \times \left\{1 + \frac{aL}{2\text{Pe}}\left(1 - e^{-2\text{Pe}}\right) + e^{aL}\left[aL - 1 + \frac{aL}{2\text{Pe}}\left(aL - 1 - \frac{aL}{2\text{Pe}}\right)\right] + aL\left(1 + \frac{aL}{2\text{Pe}}\right)\frac{e^{aL-2\text{Pe}}}{2\text{Pe}}\right\} \tag{3.16}$$

For a uniform hillslope ($a = 0$), this reduces to:

$$m_1^* = \frac{\left[2\text{Pe}^2 - 1 + (2\text{Pe} + 1)\, e^{-2\text{Pe}}\right]}{2\text{Pe}^3} \tag{3.17}$$

Equation (3.17) is consistent with the expression given in *Brutsaert* (1994, equation 24). Higher order moments can be derived in a similar manner, however their expressions are too lengthy to be given here.

3.3.3 Initial condition 2

The second type of initial condition corresponds to a storage profile derived from the steady state solution of (3.1) for a given recharge (similar to *Verhoest and Troch* 2000). This guarantees that the initial storage profile is consistent with the governing flow equation and with the boundary conditions. The steady state solution is given by

$$S_0(x) = \left(\frac{L}{2}\right)^2 \frac{N_0 c}{K}\frac{2}{aL}\left\{\frac{e^{aL}}{\frac{UL}{2K}}\left(1 - e^{-\frac{Ux}{K}}\right) + \frac{1}{\frac{aL}{2} + \frac{UL}{2K}}\left(e^{-\frac{Ux}{K}} - e^{ax}\right)\right\} \quad \forall x \in [0, L] \tag{3.18}$$

where N_0 is the recharge such that the maximum groundwater table height just reaches the ground surface (see Appendix 6.3). The dimensionless initial storage profile is given by

$$S_0^*(x^*) = \frac{N_0 c}{K}\frac{2}{aL}\left\{\frac{e^{aL}}{\text{Pe}}\left(1 - e^{-\text{Pe}\,x^*}\right) + \frac{1}{\frac{aL}{2} + \text{Pe}}\left(e^{-\text{Pe}\,x^*} - e^{\frac{aL}{2}x^*}\right)\right\} \tag{3.19}$$

The dimensionless parameter set π_0^* is $\{\frac{N_0 c}{K}; \frac{aL}{2}; \text{Pe}\}$. $\frac{N_0 c}{K}$ is a proportionality factor for S_0^* and hence for ϕ. Pe appears in π_0^* because the initial condition is the solution of the steady state differential equation, with the same geometric constraints, but it does not yield an additional

dimensionless number for $\widetilde{S^*}$ because the expression for $\widetilde{S}^*$ already contains Pe (appendix 6.1). This leads to $\pi^* = \{\frac{aL}{2}\}$. However, the fact that the two types of initial conditions produce the same parameter set π^* does not mean that the characteristic responses will be the same, because the functions ϕ_n will be different in general.

The obtained expression for the dimensionless discharge in the Laplace domain is (see Appendix 6.2.2)

$$\begin{aligned}\widetilde{Q}^*(s^*, x^*) = &- \frac{8N_0c}{K} \frac{1}{4s^* \left[aL\left(aL + 2\mathrm{Pe}\right) - 4s^*\right]} \Bigg\{ \frac{e^{aL}\left[aL\left(aL + 2\mathrm{Pe}\right) - 4s^*\right] + 4s^* e^{\frac{aL}{2}x^*}}{aL} \\ &- \frac{4s^*\left[e^{(d-b)L} e^{\frac{L(d+b)}{2}x^*} - e^{(d+b)L} e^{\frac{L(d-b)}{2}x^*}\right]}{L\left[(b-d)\, e^{(d+b)L} + (b+d)\, e^{(d-b)L}\right]} \\ &- \frac{e^{aL}\left(aL + 2\mathrm{Pe}\right) L\left[(b-d)\, e^{\frac{L(d+b)}{2}x^*} + (b+d)\, e^{\frac{L(d-b)}{2}x^*}\right]}{L\left[(b-d)\, e^{(d+b)L} + (b+d)\, e^{(d-b)L}\right]} \Bigg\}\end{aligned} \tag{3.20}$$

The dimensionless total initial volume uphill of the outlet is

$$\begin{aligned}V^* = -\widetilde{Q}^*(0,0) = \; &\frac{8N_0c}{aLK} \Bigg\{ \frac{e^{aL}}{2\mathrm{Pe}} \left[1 - \frac{1}{2\mathrm{Pe}}\left(1 - e^{-2\mathrm{Pe}}\right)\right] \\ &- \frac{1}{aL + 2\mathrm{Pe}} \left[\frac{1}{aL}\left(e^{aL} - 1\right) - \frac{1}{2\mathrm{Pe}}\left(1 - e^{-2\mathrm{Pe}}\right)\right] \Bigg\}\end{aligned} \tag{3.21}$$

This expression can also be obtained by integrating (3.13) between $x^* = 0$ and $x^* = 2$. The analytical expressions for the first and higher order dimensionless CRF moments can be derived in a similar manner as in section 3.3.2. However, their expressions are too lengthy to be given here.

3.4 Discussion

3.4.1 General behaviour of CRF moments as functions of Pe

In this section, we analyze the dimensionless moments of the CRF derived from the two types of initial conditions. As discussed before, the hillslope Péclet number is a similarity parameter for subsurface flow along complex hillslopes. In Figures 3.2 and 3.3, we present the first four dimensionless CRF central moments as function of Pe. A double-logarithmic scale is used to improve the visual inspection for advection dominated and diffusion dominated responses. The analytical solutions derived in the Laplace domain show that the dimensionless number linked to both types of initial conditions is $aL/2$. Consequently, in order to analyze the influence of the

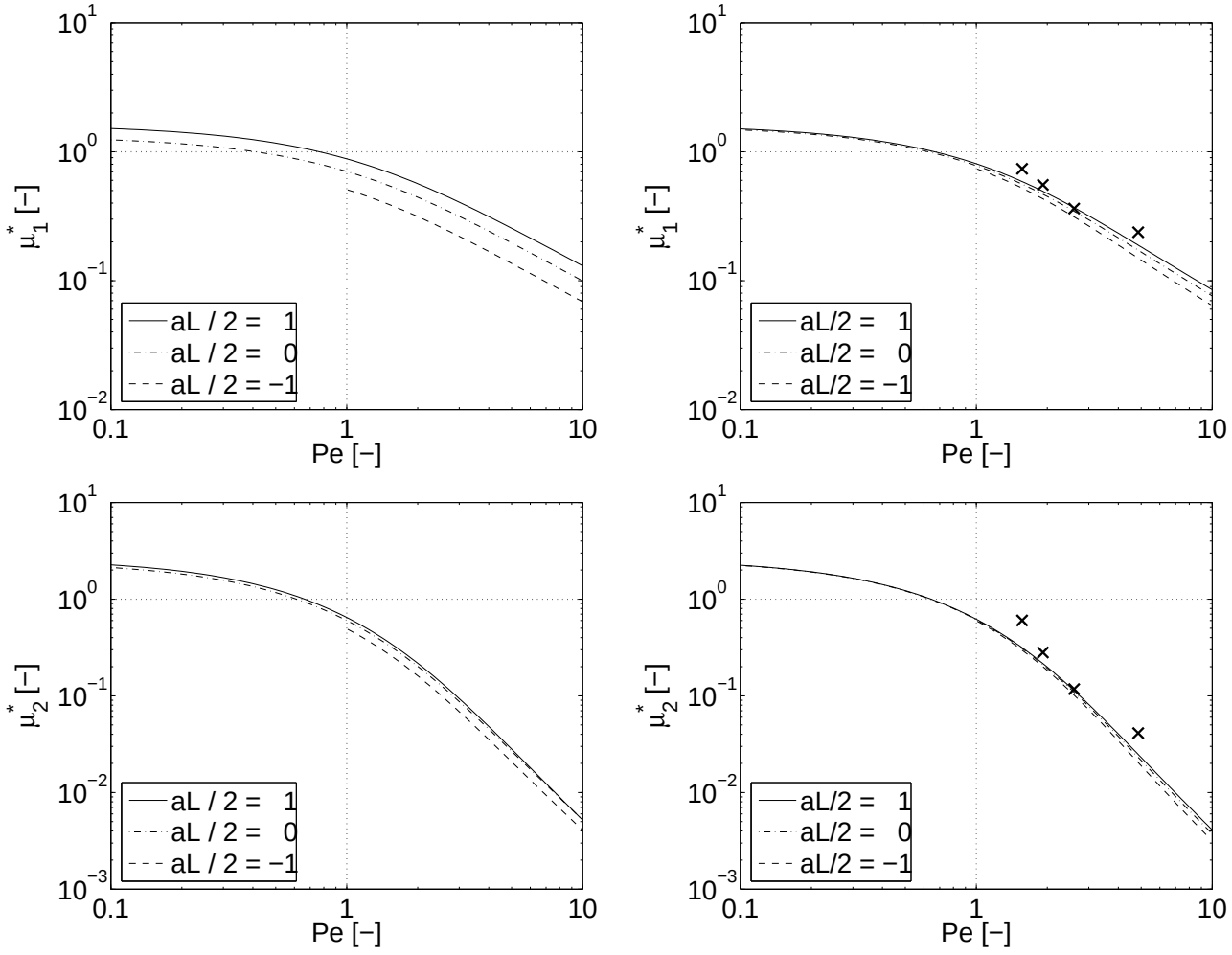

Figure 3.2: First and second dimensionless CRF central moments plotted as functions of Pe, for the first type of initial condition (left) and the second type of initial condition (right). The vertical dotted line indicates Pe = 1, and the horizontal dotted line indicates $\mu_n^* = 1$. The ($\times$) signs indicate the results from the laboratory outflow experiments.

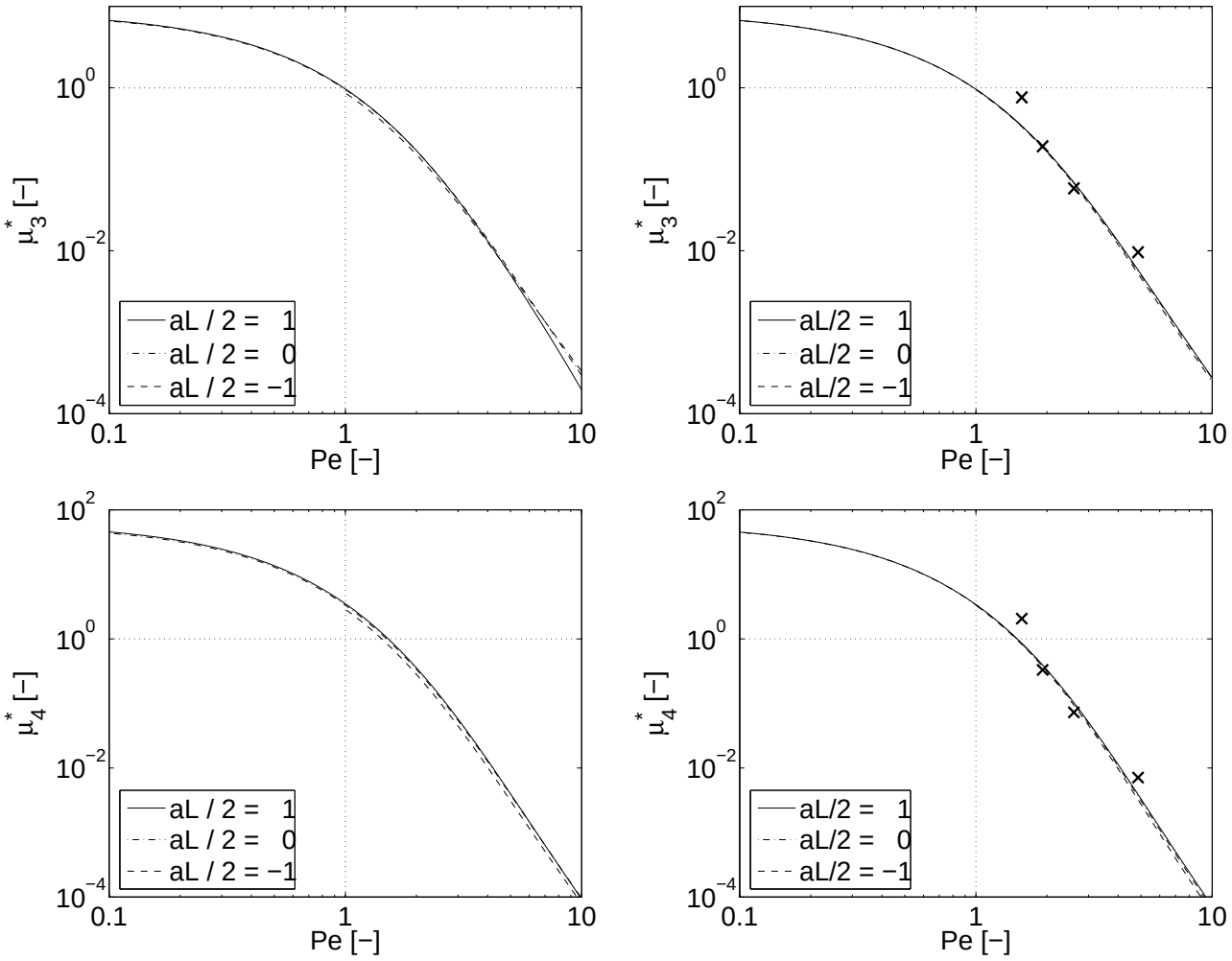

Figure 3.3: Third and fourth dimensionless CRF central moments plotted as functions of Pe, for the first type of initial condition (left) and the second type of initial condition (right). The vertical dotted line indicates Pe = 1, and the horizontal dotted line indicates $\mu_n^* = 1$. The (×) signs indicate the results from the laboratory outflow experiments.

initial condition, the moments are also plotted for three different values of $aL/2$ corresponding to a convergent ($aL/2 = +1$), a uniform ($aL/2 = 0$) and a divergent ($aL/2 = -1$) hillslope, respectively.

From Figures 3.2 and 3.3, it is clear that the curves representing the relation between the dimensionless central moments and Pe are similar for the two types of initial conditions and the investigated values of $aL/2$. This indicates that Pe is an efficient similarity parameter to define the hillslope subsurface flow response. The shape of the curves for a given moment suggests different asymptotic behaviour for the pure diffusion (Pe $\rightarrow 0$) and pure advection (Pe $\rightarrow +\infty$) case. When both processes are more or less in balance (Pe ~ 1), there is a transition zone. It is interesting to observe that these curves are almost overlapping for distinct values of $aL/2$, except for the first moment and the first type of initial condition. This shows that, in this case, the function ϕ_1 is sensitive to $aL/2$.

For both types of initial conditions, the evolution of the first four dimensionless CRF moments with Pe is similar. When Pe increases and therefore the contribution of the diffusion term becomes less important, the dimensionless moments decrease and the higher the order of the moment, the faster the decrease. We can also observe in Figures 3.2 and 3.3 that at Pe values close to 1, the dimensionless central moments assume values around 1, hence the time scales of the moments are of the order of the characteristic times of the diffusive and advective processes.

We can further study the influence of the separate hillslope parameters on the CRF moments. First we focus on the hydraulic parameters. As Pe and the π^* set from the studied types of initial conditions are independent of the hydraulic parameters f and k, the dimensionless central moments of the CRF are not affected by the variations of the hydraulic parameters. Equation (3.10) implies that τ_K is proportional to f and to $1/k$. Therefore, the dimensional central moments μ_n are proportional to f^n and to k^{-n}.

Next, we study the influence of the geometric parameters. As explained in section 3.2.2, Pe is function of three dimensionless numbers linked to the bedrock slope ($\tan\alpha$), to the aquifer length/depth ratio ($L/(2pD)$), and to the plan shape ($aL/2$). Equation (3.8) shows that Pe increases with $L/(2pD)$ ($\tan\alpha$ respectively). Hence μ_n^* decreases when the hillslope soil mantle becomes thinner (steeper respectively). When the effect of the initial condition is limited (in particular for the second type), the influence of the plan shape can be directly deduced from Figures 3.2 and 3.3. When $aL/2$ increases, Pe decreases and therefore μ_n^* increases. As τ_K is independent of $aL/2$, μ_n increases when $aL/2$ increases, keeping all other parameters fixed.

3.4.2 Comparison with experimental data

The similarity analysis described above can be tested with outflow measurements for different hillslope types during free drainage experiments. *Hilberts et al.* (2005) report such data from

hillslope experiments conducted at the Hydraulics Laboratory of the Hydrology and Quantitative Water Management group at Wageningen University. During these experiments 6 hillslope configurations were used: 2 plan shapes (linearly convergent and linearly divergent) and 3 bedrock slopes (5%, 10%, and 15%). Each hillslope was brought to steady state by means of a rainfall generator applying a constant rain rate. The boundary conditions during these experiments correspond to those assumed in the derivation of the analytical expressions for the CRF moments (Section 3.3.1). The initial conditions compare to our second type of initial condition: a steady state saturated storage profile corresponding to a constant recharge N. When the constant rain rate was stopped, the outflow and the saturated storage changes were measured with 10 minute time intervals. For more details about this experiment we refer to *Hilberts et al.* (2005).

The length L of the hillslopes was 6 m. The hydraulic conductivity k of the sandy soil used in the experiments was estimated, on soil cores, at 40 m day^{-1}. The drainable porosity values were taken from *Hilberts et al.* (2005), who computed them as the ratio between the total outflow volume and the total soil volume (pore volume plus solid matrix). For the exponential width function, the parameter c was taken as the outlet width and the degree of convergence a was adjusted in order to preserve the experimental hillslope area, $A = c(e^{aL} - 1)/a$. The initial recharge rate N_0 was derived from the measured outflow at $t = 0$ (Appendix 6.1, equation 6.24). The linearization parameter p was treated as a fitting parameter (e.g. *Brutsaert* 1994). For each hillslope, a value of p was derived (numerically) such that the theoretical total outflow volume given in (3.21) was equal to the measured total outflow volume. However, for the convergent hillslopes with 5% and 10% slopes, the obtained p values were not realistic ($p > 1$). Therefore, we could not derive the experimental CRF moments in these two cases. Our estimation of p is sensitive to uncertainties affecting the hillslope characteristics (in particular the width function and the hydraulic properties) and the recharge applied to reach the steady state. Based on these geometric and hydraulic parameters, the hillslope Peclet number (Pe) and the characteristic diffusive time (τ_K) were computed (Table 3.1).

The range of Pe values is from 1.56 to 4.86 (in the moderate advective regime) and the range of τ_K values is from 6.5 to 16.1 hours. After normalizing the observed hydrographs during each free drainage experiment, the first four dimensionless empirical moments of the CRF were calculated and plotted in Figures 3.2 and 3.3. Note the close agreement with the theoretical dimensionless moments. The functional dependence of these moments on Pe is well preserved for all four moments. The difference between the empirical and theoretical moments is small, especially if we consider the effect of measurement errors, the effect of linearization of the governing dynamic equation, the imposed exponential plan shape (which in reality is linear), and the uncertainties related to the determination of p. This illustrates that the proposed similarity parameter Pe allows, at least to first order, to predict the CRF of hillslopes with complex geometry.

As the linearization parameter p influences Pe and τ_K, its estimation is an important ques-

Table 3.1: Parameter Values for the Experimental Hillslopes (based on *Hilberts et al.* 2005).

Parameter	Convergent	Divergent			Unit
Slope ($\tan\alpha$)	0.15	0.05	0.10	0.15	-
Soil depth D	0.48	0.44	0.44	0.44	m
Drainable porosity f	0.23	0.18	0.26	0.31	-
Width at the outlet c	0.5	2.5	2.5	2.5	m
Degree of convergence a	0.31	-0.185	-0.185	-0.185	m^{-1}
Initial recharge rate N_0	21.4	17.7	25.9	31.7	mm h^{-1}
Linearization parameter p	0.16	0.34	0.50	0.50	-
Hillslope Péclet number Pe	4.86	1.56	1.92	2.60	-
Characteristic diffusive time τ_K	16.1	6.5	6.5	7.7	h

tion. We estimate the value of p by matching the total outflow volume, but other optimization strategies are possible (fitting the experimental storage profile for example). The issue of the estimation of p is subject of ongoing research.

3.5 Conclusions

This chapter reports the results of an analytical similarity study of subsurface flow response along complex hillslopes. Our similarity analysis is based on an exact analytical solution of an advection-diffusion equation, derived from a linearized form of the governing equation, in the Laplace domain. This solution is employed as the moment generating function of the characteristic response function in order to derive analytical expressions for the moments as functions of the hydraulic and geometric hillslope properties.

By means of a dimensional analysis, we show that the effects of the hillslope properties and those of the boundary and initial conditions can be separated. In a dimensionless formulation, one similarity parameter is sufficient to describe the characteristic subsurface flow response, apart from the influence of the boundary and initial condition. This number depends only on the geometric characteristics of the hillslope and is referred to as the hillslope Péclet number. It accounts for the relative importance of the diffusion and advection terms.

Given fixed boundary conditions, we demonstrated the consistency of the global behaviour of the CRF moments for both types of initial conditions. The initial condition has a significant influence on the low order moments, when the initial volume of water is uniformly distributed over the hillslope (first type of initial condition). On the contrary, the initial condition has a limited impact when the initial storage profile corresponds to a steady state storage profile (second type of initial condition). Therefore, in this case, the hillslope Péclet number almost completely describes the dimensionless CRF moments. Because we consider a spatially

distributed system, the position within the hillslope is important and many different initial conditions can be defined. Therefore, care should be taken to use the CRF obtained from an arbitrary initial condition in a convolution operation to compute the hillslope subsurface flow response during time-varying recharge.

Outflow measurements from an experimental hillslope in four different configurations offered the opportunity to test our approach. The confrontation of the theoretical and empirical values of the dimensionless moments of the CRF shows that the derived analytical expressions provide the relevant order of magnitude.

The validity of our results is restricted to (i) the validity domain of the hsB equation (shallow soil mantle, stream lines parallel to the impervious bedrock, negligible influence of the unsaturated zone and absence of overland flow), (ii) the validity domain of the linearization (constant slope angle, uniform hydraulic parameters and storage profile close to the mean profile), and (iii) the considered boundary conditions.

Further research is being carried out to validate the hillslope Péclet number as hillslope subsurface flow similarity parameter by confrontation with other experimental data. As previously mentioned, the estimation of the linearization parameter is an important issue for the applicability of the approach and hence must be studied. Finally, our analysis has been conducted at the hillslope scale and the scaling from hillslopes to catchments deserves further investigation.

Chapter 4

Application to real catchments

In order to assess the validity and the limits of the hsB model and the proposed similarity approach (see previous chapters), a first application to the Plynlimon catchments (*Kirchner et al.* 2000) is currently being performed. Two small catchments are studied: Tanllwyth (0.97 km^2) and Hafren (3.47 km^2). Five years of hourly rain and stream measurements are available. Three parameters are calibrated on a continuous 2-year period. Figure 2 illustrates (1) the ability of the model to correctly reproduce the temporal dynamics and the amplitude of the discharge at the outlet, but also (2) the poor performance for low flow periods, during which the base flow due to the groundwater contribution is predominant and not taken into account in the model. These results are preliminary and further results will be reported at a later stage.

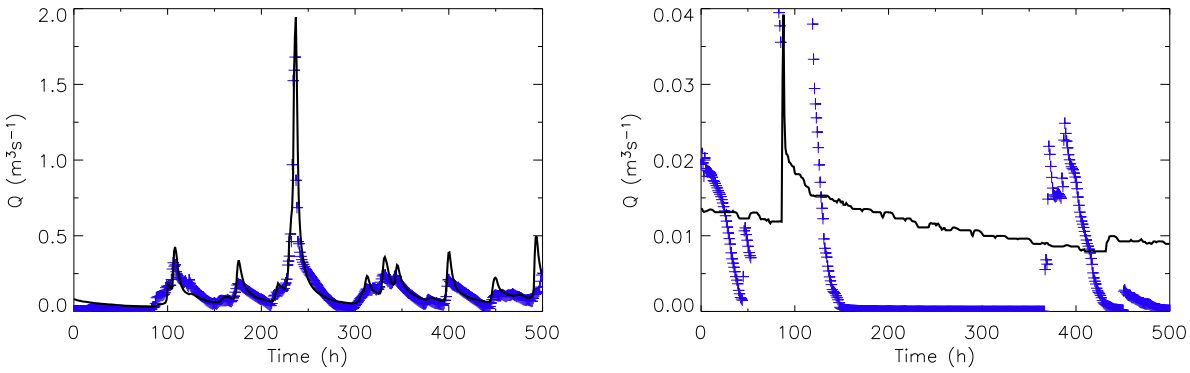

Figure 4.1: Examples of comparison between observed (solid line) and simulated (+) discharges during (left pannel) a high flow period and (right pannel) a low flow period.

Chapter 5

Conclusions

The main results of previous chapters are briefly summarized in the following:

- Introducing the width function and the groundwater storage of the hillslope in the Boussinesq equation leads to the hillslope-storage Boussinesq equation (hsB). This equation describes the diffusion and advection components of the subsurface flow and takes the three-dimensional aspect of the hillslope explicitly into account.

- A similarity parameter, called the hillsope Péclet number, has been derived from a dimensional analysis of a linearized version of the hsB equation. This approach offers an interesting potential for studying the hydrology of ungauged basins.

- The first application of the hsB approach to real catchments has been performed in the Plynlimon region (Wales). For small catchments (a few km^2), the model is able to reproduce the discharge signal (in terms of dynamics and volume) during high flow periods, but the model performs poorly during low flow periods because of, in this case, the significant influence of the deep groundwater system which is not taken into account in the hsB approach.

Finally, the results presented in this report open potentially fruitful research directions for small catchment hydrology in an ungauged context.

Bibliography

Aryal, S., E. O'Loughlin, and R. Mein (2002), A similarity approach to predict landscape saturation in catchments, *Water Resour. Res.*, *38*(10), 1208, doi:10.1029/2001WR000864.

Beven, K., and M. Kirkby (1979), Towards a simple, physically based, variable contributing area model of basin hydrology, *Hydrol. Sci. Bull.*, *24*(1), 43–69.

Boyce, W., and R. DiPrima (1977), *Elementary differential equation and boundary value problems*, 3rd ed., 582 pp., John Wiley and Sons.

Bronstert, A. (1994), 1-, 2-, and 3-dimensional modeling of the water dynamics of agricultural sites using a physically based modeling system "Hillflow", in *2nd European Conference on Advances in Water Resources Technology and Management*, edited by Tsakiris and Santos, pp. 43–69.

Brutsaert, W. (1994), The unit response of groundwater outflow from a hillslope, *Water Resour. Res.*, *30*(10), 2759–2763.

Buckingham, E. (1914), On physically similar systems; illustrations of the use of dimensional equations, *Phys. Rev.*, *4*, 345–376.

Chapman, T. (1995), Comment on "The unit response of groundwater outflow from a hillslope" by Wilfried Brutsaert, *Water Resour. Res.*, *31*(9), 2377–2378.

Dooge, J. (1973), Linear theory of hydrologic systems, *Tech. Bull. 1468*, Agric. Res. Serv., U.S. Dep. of Agric., Washington, D.C.

Dunne, T., and R. Black (1970), An experimental investigation of runoff production in permeable soils, *Water Resour. Res.*, *6*(2), 478–490.

Fan, Y., and R. Bras (1998), Analytical solutions to hillslope subsurface storm flow and saturation overland flow, *Water Resour. Res.*, *34*(2), 921–927.

Freeze, R. (1972a), Role of subsurface flow in generating surface runoff: 1. Base flow contributions to channel flow, *Water Resour. Res.*, *8*(3), 609–623.

Freeze, R. (1972b), Role of subsurface flow in generating surface runoff: 2. Upstream source areas, *Water Resour. Res.*, *8*(5), 1272–1283.

Hebson, C., and E. Wood (1986), On hydrologic similarity: 1. Derivation of the dimensionless flood frequency curve, *Water Resour. Res.*, *22*(11), 1549–1554.

Hilberts, A., E. van Loon, P. Troch, and C. Paniconi (2004), The hillslope-storage Boussinesq model for non-constant bedrock slope, *J. Hydrol.*, *291*(3-4), 160–173.

Hilberts, A., P. Troch, and C. Paniconi (2005), Storage-dependent drainable porosity for complex hillslopes, *Water Resour. Res.*, *41*, W06001, doi:10.1029/2004WR003725.

Kirchner, J., X. Feng, and C. Neal (2000), Fractal stream chemistry and its implications for contaminant transport in catchments, *Nature*, *403*, 524–527.

Kirchner, J., X. Feng, and C. Neal (2001), Catchment-scale advection and dispersion as a mechanism for fractal scaling in stream tracer concentrations, *J. Hydrol.*, *254*(1-4), 82–101.

Mood, A., F. Graybill, and D. Boes (1974), *Introduction to the theory of statistics*, Statistics Series, 3rd ed., 564 pp., McGraw-Hill.

Paniconi, C., and E. Wood (1993), A detailed model for simulation of catchment scale subsurface hydrological processes, *Water Resour. Res.*, *29*(6), 1601–1620.

Paniconi, C., P. Troch, van Loon E., and A. Hilberts (2003), Hillslope-storage Boussinesq model for subsurface flow and variable source areas along complex hillslopes: 2. Intercomparison with a three-dimensional Richards equation model, *Water Resour. Res.*, *39*(11), 1317, doi: 10.1029/2002WR001730.

Rodríguez-Iturbe, I., and J. Valdés (1979), The geomorphologic structure of hydrologic response, *Water Resour. Res.*, *15*(6), 1409–1420.

Saleem, J., and G. Salvucci (2004), Comparison of soil wetness indices for inducing functional similarity of hydrologic response across sites in Illinois, *J. Hydrometeor.*, in press.

Sivapalan, M., K. Beven, and E. Wood (1987), On hydrologic similarity: 2. A scaled model of storm runoff production, *Water Resour. Res.*, *23*(12), 2266–2278.

Sivapalan, M., E. Wood, and K. Beven (1990), On hydrologic similarity: 3. Dimensionless flood frequency model using a generalized geomorphologic unit hydrograph and partial area runoff generation, *Water Resour. Res.*, *26*(1), 43–58.

Troch, P., E. van Loon, and A. Hilberts (2002), Analytical solutions to a hillslope-storage kinematic wave equation for subsurface flow, *Adv. Water Resour.*, *25*(6), 637–649.

Troch, P., E. van Loon, and C. Paniconi (2003), Hillslope-storage Boussinesq model for subsurface flow and variable source areas along complex hillslopes: 1. Formulation and characteristic response, *Water Resour. Res.*, *39*(11), 1316, doi:10.1029/2002WR001728.

Troch, P., A. van Loon, and A. Hilberts (2004), Analytical solution of the linearized hillslope-strorage Boussinesq equation for exponential hillslope width functions, *Water Resour. Res.*, *40*(8), W08601, doi:10.129/2003WR002850.

Verhoest, N., and P. Troch (2000), Some analytical solutions of the linearized Boussinesq equation with recharge for a sloping aquifer, *Water Resour. Res.*, *36*(3), 793–800.

Chapter 6

Appendices

6.1 Derivation of the dimensionless equation

The dimensionless initial storage profile is given by

$$S_0^*(x^*, \pi_0^*) = \left(\frac{L}{2}\right)^{-2} S_0 \tag{6.1}$$

where $\pi_0^* = \{\pi_1^*, ..\pi_{n_0}^*\}$ denotes the set of dimensionless parameters required to describe S_0^*. Now we define the dimensionless Laplace transform of the storage as

$$\widetilde{S}^* = \left(\frac{L}{2}\right)^{-4} K\, \widetilde{S} = \left(\frac{L}{2}\right)^{-4} K \int_0^\infty e^{-st} S(x,t)\, dt \tag{6.2}$$

Introducing these variables in (3.4) yields

$$\frac{\partial^2 \widetilde{S}^*}{\partial {x^*}^2} + \frac{UL}{2K}\frac{\partial \widetilde{S}^*}{\partial x^*} - s^* \widetilde{S}^* = -S_0^* \tag{6.3}$$

which implies that

$$\widetilde{S}^* = \psi\left(s^*, x^*, \frac{UL}{2K}, \pi_\psi^*\right) \tag{6.4}$$

where ψ is a function of dimensionless variables, and π_ψ^* denotes the set of parameters π_i^* independent of $\frac{UL}{2K}$ and the dimensionless parameters required to describe the boundary conditions. Let $\widetilde{Q}$ be the Laplace transform of the discharge and let us write (3.2) in the Laplace domain:

$$\widetilde{Q} = -K\frac{\partial \widetilde{S}}{\partial x} - U\widetilde{S} \tag{6.5}$$

Similarly, we define the dimensionless Laplace transform of the discharge $\widetilde{Q}^*$ as

$$\widetilde{Q}^* = \left(\frac{L}{2}\right)^{-3} \widetilde{Q} \tag{6.6}$$

So (6.5) becomes

$$\widetilde{Q}^* = -\frac{\partial \widetilde{S}^*}{\partial x^*} - \frac{UL}{2K}\widetilde{S}^* \tag{6.7}$$

Combining (6.4) and (6.7) yields

$$\widetilde{Q}^* = -\phi\left(s^*, x^*, \frac{UL}{2K}, \pi_\psi^*\right) \tag{6.8}$$

where ϕ is a positive function of dimensionless variables. At this stage, we have a general formulation for the dimensionless Laplace transform of the discharge. The dimensionless total volume of water initially stored in the hillslope uphill of x is given by:

$$V^*(x^*) = -\left[\widetilde{Q}^*\right]_{s^*=0} = \left[\phi\left(s^*, x^*, \frac{UL}{2K}, \pi_\psi^*\right)\right]_{s^*=0} \tag{6.9}$$

Because $\widetilde{Q}^*$ is negative, the dimensionless CRF is obtained by normalizing $-\widetilde{Q}^*$ by the dimensionless total volume at the outlet ($x^* = 0$). As the Laplace transform of the CRF is its moment generating function, we can derive a general formulation for the dimensionless CRF moments:

$$m_n^* = (-1)^{n+1}\frac{1}{V^*(0)}\left[\frac{\partial^n \widetilde{Q}^*}{\partial {s^*}^n}\right]_{s^*=0} = \phi_n\left(\frac{UL}{2K}, \pi^*\right) \tag{6.10}$$

where m_n^* denotes the dimensionless n$^{\text{th}}$ order moment and π^* represents the subset of dimensionless parameters from π_ψ^* that remain after the normalization. ϕ_n is defined as

$$\phi_n = \frac{(-1)^n}{V^*(0)}\left[\frac{\partial^n \phi}{\partial {s^*}^n}\left(s^*, x^*, \frac{UL}{2K}, \pi_\psi^*\right)\right]_{\{s^*, x^*\}=\{0,0\}} \tag{6.11}$$

According to (6.9) and (6.11), any proportionality factor of ϕ will disappear in ϕ_n. This property is applied in section 3.3.

6.2 Derivation of an analytical solution in the Laplace domain

For a given s, (3.4) is a linear ordinary differential equation (ODE) with constant coefficients and non-homogeneous forcing term. The solution of such an ODE is given as the sum of the solution ($\widetilde{S}_h$) of the corresponding homogeneous ODE and a particular solution ($\widetilde{S}_p$). The general solution of the homogeneous equation is:

$$\widetilde{S}_h(s, x) = C_1 e^{(d+b)x} + C_2 e^{(d-b)x} \tag{6.12}$$

where

$$d = -\frac{U}{2K}$$
$$b = \sqrt{d^2 + \frac{s}{K}}$$

C_1 and C_2 are constants and their values are chosen such as to satisfy the boundary conditions. Both (C_1, C_2) and the particular solution (derived using the method of variation of parameters, e.g. *Boyce and DiPrima* 1977) depend on the assumed initial condition, through the forcing term S_0.

6.2.1 Initial condition 1

The particular solution is

$$\widetilde{S}_p = -\frac{\gamma D f c}{Ka^2 + Ua - s} e^{ax} \tag{6.13}$$

So the general solution is

$$\widetilde{S}(s,x) = C_1 e^{(d+b)x} + C_2 e^{(d-b)x} - \frac{\gamma D f c}{Ka^2 + Ua - s} e^{ax} \tag{6.14}$$

where C_1 and C_2 are calculated in order to satisfy the boundary conditions (3.11):

$$\begin{aligned} C_1 &= \frac{\gamma D f c}{Ka^2 + Ua - s} \; \frac{e^{aL}(a-2d) + e^{(d-b)L}(d+b)}{(b-d)\, e^{(d+b)L} + (b+d)\, e^{(d-b)L}} \\ C_2 &= \frac{\gamma D f c}{Ka^2 + Ua - s} \; \frac{e^{(d+b)L}(b-d) - e^{aL}(a-2d)}{(b-d)\, e^{(d+b)L} + (b+d)\, e^{(d-b)L}} \end{aligned} \tag{6.15}$$

Using (3.2) we can derive the expression for the discharge dynamics in the Laplace domain:

$$\begin{aligned} \widetilde{Q}(s,x) = -\, L^3 \, \frac{\gamma D f c}{L^2} \, \frac{1}{\left(aL(aL + 2\mathrm{Pe}) - s\frac{L^2}{K}\right)} \Bigg\{ & - e^{ax} \left(aL + 2\mathrm{Pe}\right) \\ & + \frac{s\frac{L^2}{K}\left[e^{(d-b)L} e^{(d+b)x} - e^{(d+b)L} e^{(d-b)x}\right]}{L\left[(b-d)\, e^{(d+b)L} + (b+d)\, e^{(d-b)L}\right]} \\ & + \frac{\left(aL + 2\mathrm{Pe}\right) L e^{aL}\left[(b-d)\, e^{(d+b)x} + (b+d)\, e^{(d-b)x}\right]}{L\left[(b-d)\, e^{(d+b)L} + (b+d)\, e^{(d-b)L}\right]} \Bigg\} \end{aligned} \tag{6.16}$$

As $dL = -\mathrm{Pe}$ and $bL = \sqrt{Pe^2 + 4s^*}$, (6.16) can be expressed in the form of (6.8).

6.2.2 Initial condition 2

The particular solution of (3.4) is derived using to the initial storage profile given in (6.21):

$$\widetilde{S}_p = \frac{N_0 c}{a}\left[\frac{e^{aL}}{sU}\left(1-e^{-\frac{U}{K}x}\right)+\frac{1}{(Ka+U)}\left(\frac{e^{-\frac{U}{K}x}}{s}+\frac{e^{ax}}{Ka^2+Ua-s}\right)\right] \tag{6.17}$$

So the general solution is

$$\begin{aligned}\widetilde{S}(s,x) = \; & \frac{N_0 c}{a}\left[\frac{e^{aL}}{sU}\left(1-e^{-\frac{U}{K}x}\right)+\frac{1}{(Ka+U)}\left(\frac{e^{-\frac{U}{K}x}}{s}+\frac{e^{ax}}{Ka^2+Ua-s}\right)\right] \\ & + C_1 e^{(d+b)x} + C_2 e^{(d-b)x}\end{aligned} \tag{6.18}$$

and C_1 and C_2 are

$$\begin{aligned}C_1 &= -\frac{N_0 c}{s\left(Ka^2+Ua-s\right)}\frac{e^{aL}(a+\frac{U}{K})+e^{(d-b)L}(d+b)}{(b-d)\,e^{(d+b)L}+(b+d)\,e^{(d-b)L}} \\ C_2 &= -\frac{N_0 c}{s\left(Ka^2+Ua-s\right)}\frac{e^{(d+b)L}(b-d)-e^{aL}(a+\frac{U}{K})}{(b-d)\,e^{(d+b)L}+(b+d)\,e^{(d-b)L}}\end{aligned} \tag{6.19}$$

Similarly, the expression for the discharge in the Laplace domain is derived using (3.2):

$$\begin{aligned}\widetilde{Q}(s,x) = & -L^3\frac{N_0 c}{K}\frac{1}{s\frac{L^2}{K}\left[aL\left(aL+2\mathrm{Pe}\right)-s\frac{L^2}{K}\right]}\left\{\frac{e^{aL}\left[aL\left(aL+2\mathrm{Pe}\right)-s\frac{L^2}{K}\right]+s\frac{L^2}{K}e^{aL\frac{x}{L}}}{aL}\right. \\ & -\frac{e^{aL}\left(aL+2\mathrm{Pe}\right)L\left[(b-d)\,e^{L(d+b)\frac{x}{L}}+(b+d)\,e^{L(d-b)\frac{x}{L}}\right]}{L\left[(b-d)\,e^{(d+b)L}+(b+d)\,e^{(d-b)L}\right]} \\ & \left.-\frac{s\frac{L^2}{K}\left[e^{(d-b)L}e^{L(d+b)\frac{x}{L}}-e^{(d+b)L}e^{L(d-b)\frac{x}{L}}\right]}{L\left[(b-d)\,e^{(d+b)L}+(b+d)\,e^{(d-b)L}\right]}\right\}\end{aligned} \tag{6.20}$$

Equation (6.20) can also be expressed in the form of (6.8).

6.3 Derivation of the initial steady state solution

We derive the steady state solution of (3.1) for a given recharge N:

$$S_0 = \frac{Nc}{a}\left[\frac{e^{aL}}{U}\left(1-e^{-\frac{U}{K}x}\right)+\frac{1}{(Ka+U)}\left(e^{-\frac{U}{K}x}-e^{ax}\right)\right] \tag{6.21}$$

In order to define a unique initial condition, we have to fix a value for N. We use the recharge such that the maximum mean (over the hillslope width) groundwater table height $\overline{h}_m$ along the

hillslope just reaches the ground surface. We must first calculate the maximum mean groundwater table height as a function of N and then determine N_0 such that $\overline{h}_m = D$.

According to the definition of the storage S, the mean groundwater table height is

$$\overline{h} = \frac{S}{fw} = \frac{Ne^{-ax}}{af}\left[\frac{e^{aL}}{U}\left(1 - e^{-\frac{U}{K}x}\right) + \frac{1}{Ka+U}\left(e^{-\frac{U}{K}x} - e^{ax}\right)\right] \tag{6.22}$$

We want to calculate the x-coordinate x_m where the mean groundwater table height is maximum. Solving $\overline{h}'(x_m) = 0$, where the prime denotes a derivative with respect to x, yields

$$x_m = \frac{K}{U}\ln\left[1 + \frac{U}{Ka}\left(1 - e^{-aL}\right)\right] \tag{6.23}$$

For uniform hillslope ($a = 0$), this reduces to $x_m = \frac{K}{U}\ln(1 + \frac{UL}{K})$, which is consistent with *Verhoest and Troch* (2000, equation 21). It is easy to check that $x = x_m$ corresponds to a maximum. To derive a simple expression for $\overline{h}(x_m)$, we must note that the discharge expression is simple in the steady state. Integrating the continuity equation leads to

$$Q(x) = -\int_x^L Nw(u)\,du = \frac{Nc}{a}\left(e^{ax} - e^{aL}\right) \tag{6.24}$$

From (6.22), we can also write

$$\overline{h}' = \frac{e^{-ax}}{cf}\left(S' - aS\right)$$

So

$$S'(x_m) = aS(x_m) \tag{6.25}$$

Introducing (6.25) in (3.2) yields

$$S(x_m) = -\frac{Q(x_m)}{aK+U} \tag{6.26}$$

So we obtain the following expression for the maximum mean groundwater table height:

$$\overline{h}(x_m) = \frac{N}{fa\left(aK+U\right)}\left\{e^{aL}\left[1 + \frac{U}{aK}\left(1 - e^{-aL}\right)\right]^{-\frac{aK}{U}} - 1\right\} \tag{6.27}$$

This expression can also be obtained by substituting (6.23) directly into (6.22). We can finally derive the expression of the recharge N_0 that leads to the maximum mean groundwater table height equal to D:

$$N_0 = \frac{faD\left(aK+U\right)}{e^{aL}\left[1 + \frac{U}{aK}\left(1 - e^{-aL}\right)\right]^{-\frac{aK}{U}} - 1} \tag{6.28}$$